

Comments on “Isentropic Analysis of a Simulated Hurricane”

by Pascal Marquet.

Météo-France, CNRM/GMAP-CNRS UMR-3589. Toulouse. France.

E-mail: pascal.marquet@meteo.fr

Submitted to the *Journal of Atmospheric Science* (13 July 2016).

1 Introduction

In a recent paper, Mrowiec et al. (2016, hereafter MPZ) investigated the thermodynamic properties of a three-dimensional hurricane simulation. The paper MPZ focused on isentropic analysis based on the conditional averaging of the mass transport with respect to the equivalent potential temperature θ_e , with the underlying assumption that θ_e defined in Emanuel (1994, hereafter E94) is a logarithmic measurement of the moist-air entropy. It was also assumed that isentropic surfaces are represented by constant values of θ_e .

Many other equivalent potential temperatures exist in the literature however and it is shown in this comment that the way in which the moist entropy s and these equivalent potential temperatures are defined may lead to opposite results in studies of isentropic processes in hurricanes. It is shown that the more the total water varies with space the more the isentropes differ.

The paper is organized as follows. Different potential temperatures are recalled in section 2 and the associated moist-air entropy is presented in section 3. A data-set derived from a simulation of the hurricane DUMILE is presented in section 4. Section 5 provides numerical evaluations for θ_e , θ_{es} (the saturated version of θ_e) and θ_s defined by Marquet (2011, hereafter M11), where θ_s is computed by applying the third law of thermodynamic, a process improved by Marquet (2015, 2016). Differences in the associated moist-air entropies are described in section 6, together with an evaluation of the heat input computed for a Carnot cycle in the so-called temperature-entropy diagram. A conclusion is presented in section 7.

2 The moist-air potential temperatures

The equivalent potential temperature θ_e defined by Eq. (4.5.11) in Emanuel (1994) can be written as

$$\theta_{e/E94} = T \left(\frac{p_0}{p_d} \right)^{R_d/c_{pl}^*} \exp \left(\frac{L_v r_v}{c_{pl}^* T} \right) (H_l)^{-R_v r_v/c_{pl}^*}, \quad (1)$$

where T is the temperature, p_0 is the standard pressure, p_d is the dry-air pressure, and R_d and R_v are the gas constant of water vapor and dry air, respectively. The specific heat $c_{pl}^* = c_{pd} + r_t c_l$ depends on the values for dry air (c_{pd}) and liquid water (c_l). The mixing ratios r_v and r_t represent water vapor and total water, respectively. L_v is the latent

heat of vaporization. The relative humidity with respect to liquid water $H_l = e/e_{sw}$ is the ratio of water vapor pressure (e) over the saturated value (e_{sw}).

The saturated equivalent potential temperature studied in Emanuel (1986, hereafter E86) will be written as

$$\theta_{es/E86} = T \left(\frac{p_0}{p} \right)^{R_d/c_{pl}^*} \exp \left(\frac{L_v r_{sw}}{c_{pl}^* T} \right), \quad (2)$$

where p is the total pressure and $r_{sw}(T, p)$ is the saturation mixing ratio at temperature T and pressure p .

The equivalent potential temperature studied in Betts (1973, hereafter B73) can be written as

$$\theta_{e/B73} = \theta \exp \left(\frac{L_v q_v}{c_{pd} T} \right), \quad (3)$$

where the dry-air potential temperature is $\theta = T (p_0/p)^\kappa$ with $\kappa = R_d/c_{pd} \approx 0.286$.

The equivalent potential temperature θ_e studied in MPZ can be written as

$$\theta_{e/MPZ} = T \left(\frac{p_0}{p} \right)^{R_d/c_{pl}^*} \exp \left(\frac{L_v r_v}{c_{pl}^* T} \right) (H_l)^{-R_v r_v/c_{pl}^*}. \quad (4)$$

The difference between $\theta_{e/MPZ}$ and $\theta_{e/E94}$ given by Eq. (1) is p_d replaced by p in the Exner function. The differences between $\theta_{e/MPZ}$ and $\theta_{e/E86}$ given by Eq. (2) are r_{sw} replaced by r_v and the additional term depending on H_l included. The differences between $\theta_{e/MPZ}$ and $\theta_{e/B73}$ given by Eq. (3) are c_{pd} replaced by c_{pl}^* , q_v replaced by r_v and the additional term depending on H_l included.

The third-law based potential temperature defined in Marquet (2011, 2016) can be written as

$$\begin{aligned} \theta_{s/M11} = & \theta \exp \left(- \frac{L_v q_t + L_s q_i}{c_{pd} T} \right) \exp(\Lambda_r q_t) \\ & \left(\frac{T}{T_r} \right)^\lambda \left(\frac{p}{p_r} \right)^{-\kappa \delta q_t} \left(\frac{r_r}{r_v} \right)^\gamma \frac{(1 + \eta r_v)^\kappa (1 + \delta q_t)}{(1 + \eta r_r)^\kappa \delta q_t} \\ & (H_l)^\gamma q_t (H_i)^\gamma q_i \left(\frac{T_l}{T} \right)^{c_l q_t/c_{pd}} \left(\frac{T_i}{T} \right)^{c_i q_i/c_{pd}}, \quad (5) \end{aligned}$$

where $\lambda = c_{pv}/c_{pd} - 1 \approx 0.837$, $\eta = R_v/R_d \approx 1.608$, $\delta = \eta - 1 \approx 0.608$ and $\gamma = R_v/c_{pd} \approx 0.46$. The term $\Lambda_r = [(s_v)_r - (s_d)_r]/c_{pd} \approx 5.87$ depends on the third-law values for the reference entropies for water vapor and dry air, and

L_s is the latent heat of sublimation. The specific contents q_v , q_l , q_i and $q_t = q_v + q_l + q_i$ replace the mixing ratios involved in most of the previous formulations.

The four terms in the last line of Eq. (5) derived in Marquet (2016) are improvements with respect to Marquet (2011). They take into account possible non-equilibrium processes such as under- or super-saturation with respect to liquid water ($H_l \neq 1$) or ice ($H_i \neq 1$), temperatures of rain T_l or snow T_i which may differ from those T of dry air and water vapor.

The advantage of the term $(H_l)^{\gamma q_t}$ in Eq. (5) compared with $(H_l)^{-R_v r_v/c_{pl}^*}$ in Eqs. (1) or (4) is that q_l replaces r_v in the exponent, making no impact in clear-air, under- or super-saturated moist regions (where $H_l \neq 1$ and r_v may be large, but where $q_l = 0$) and making lesser impact in cloud in under- or super-saturated regions (where $H_l \neq 1$ but where typically $q_l \ll r_v$).

The first and second order approximations of θ_s are derived in Marquet (2015), leading to

$$(\theta_s)_1 \approx \theta \exp\left(-\frac{L_v q_l + L_s q_i}{c_{pd} T}\right) \exp(\Lambda_r q_t), \quad (6)$$

$$(\theta_s)_2 \approx (\theta_s)_1 \exp[-\gamma (q_l + q_i)] \left(\frac{r_v}{r_*}\right)^{-\gamma q_t}, \quad (7)$$

where $r_* \approx 0.0124 \text{ kg kg}^{-1}$. Both $(\theta_s)_1$ and $(\theta_s)_2$ must be multiplied by the last line of Eq. (5) if non-equilibrium processes are to be described.

3 The moist-air entropies

The moist-air entropy is computed in M11 from the third-law of thermodynamics. It can be written as

$$s(\theta_{s/M11}) = s_{\text{ref}} + c_{pd} \ln(\theta_s), \quad (8)$$

$$s(\theta_{s/M11})/q_d = [s_{\text{ref}}/q_d] + [c_{pd}/q_d] \ln(\theta_s), \quad (9)$$

where both $s_{\text{ref}} \approx 1139 \text{ J K}^{-1} \text{ kg}^{-1}$ and c_{pd} are constant, making θ_s a true equivalent of the specific moist-air entropy s . The second formulation $s(\theta_{s/M11})/q_d$ is expressed “per unit of dry air”, in order to be better compared with the entropies computed in other studies such as E94 or MPZ.

Other definitions of “moist-air entropy” are derived with either s_{ref} or c_{pd} (often both of them) depending on the total-water mixing ratio r_t . This is true in Eq. (4.5.10) in E94, which can be written as

$$s(\theta_{e/E94})/q_d = [-R_d \ln(p_0)] + c_{pl}^* \ln(\theta_{e/E94}), \quad (10)$$

where p_0 is a constant standard value. The division of s by q_d means that the entropy in Eq. (10) is expressed “per unit mass of dry air”. The reference values of entropies disagree in E94 with the third law, the consequence being that several terms are missing or are set to zero in Eq. (10). These missing terms may impact the specific entropy if q_t varies in space or time, since these missing terms must be

multiplied by $q_d = 1 - q_t$ to compute s from s/q_d given by Eq. (10). Moreover, since $c_{pl}^* = c_{pd} + r_t c_l$ depends on r_t , changes in s and s/q_d cannot be represented by $\theta_{e/E94}$ in Eq. (10) for varying values of r_t . This prevents $\theta_{e/E94}$ from being a true equivalent of the specific moist-air entropy s for hurricanes, where properties of saturated regions (large values of r_t) are to be compared with non-saturated ones (small values of r_t).

Similarly, the moist-air entropy defined in section 3 in MPZ can be written as

$$s(\theta_{e/MPZ})/q_d = [-c_{pl}^* \ln(T_0)] + c_{pl}^* \ln(\theta_{e/MPZ}), \quad (11)$$

where T_0 is a constant standard value. Again, it is an entropy expressed “per unit mass of dry air” and the specific heat c_{pl}^* depends on varying values of r_t , twice preventing $\theta_{e/MPZ}$ from being a true equivalent of the specific moist entropy.

It is shown in Marquet and Geleyn (2015, section 5.3) that the linear combination $s_a = (1 - a) s(\theta_e) + a s(\theta_l)$ described in the Appendix C of Pauluis et al. (2010) can lead to the third law value of entropy $s(\theta_{s/M1})$ if the weighting factor is set to the value $a \approx 0.356$. Another value for a would lead to a definition of the specific moist-air entropy s_a which would disagree with the third law.

In order to better analyze the impact of r_t on the term c_{pl}^* , and thus on the definition of the moist-air entropy, two kinds of “saturated equivalent entropy” are defined. They are based on the definition of $\theta_{es/E86}$ given by Eq. (2), yielding

$$s(\theta_{es/E86})/q_d = c_{pl}^* \ln(\theta_{es/E86}), \quad (12)$$

$$s(\theta_{es/E86})/q_d = c_{pd} \ln(\theta_{es/E86}). \quad (13)$$

4 The data set for the hurricane DUMILE

On January 3, 2013 at 00 UTC, the hurricane Dumile was located northwest of the Réunion island and east of Madagascar, near 18.5 south latitude and 54.25 east longitude. Two cross sections are depicted in Figs. 1 and 2 for the pseudo-adiabatic potential temperature θ'_w and the relative humidity H_l . The use of θ'_w allows a clear, unambiguous definition of thermal properties, differing from the uncertain and multiple definitions of θ_e recalled in section 2 which are to be compared in later sections.

The pressure is used as a vertical coordinate and the black regions close to 1000 hPa represent the east coast of Madagascar on the left, the center of Dumile on the right. The west-east cross sections are plotted for a 12 hour forecast by employing the French model ALADIN, with a resolution of about 8 km.

The eyewall and the core of the hurricane are similar to Figs. 16 and 12 (top) plotted in Hawkins and Imbembe (1976) for the hurricane Inez, where θ_e was likely computed as an equivalent for θ'_w . The same high values of θ'_w observed

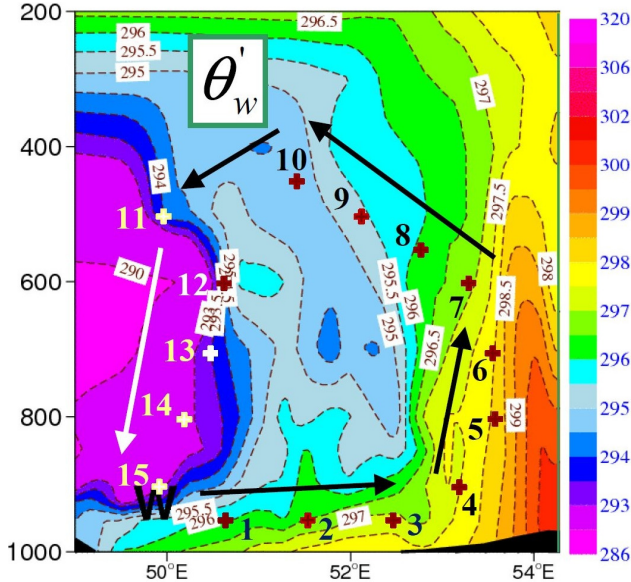


Figure 1: A pressure-longitude cross section at 18.5 south latitude for the hurricane Dumile and for the pseudo-adiabatic potential temperature θ'_w in K. The 15 points are used to build the Table 1 and to plot the Figs. 5-6.

in the eye of Inez are simulated in Fig. 1 for Dumile at the lower and upper levels. The same area of minimum θ'_w and lower relative humidity is observed in the core in the 500 to 700 layer.

The cross section depicted in Fig. 4 for θ_s exhibits great differences in comparison with Fig. 1 valid for θ'_w and with Fig. 3 valid for $\theta_{e/B73}$: there is a minimum of θ_s close to the surface in the core region; at a distance from the center θ_s exhibits a mid-tropospheric minimum at about 750 hPa while it is about 1000 m higher for θ'_w in Fig. 1, for $\theta_{e/MPZ}$ in Fig. 2a of MPZ and for $\theta_{e/B73}$ in Fig. 3; the isentropes computed and plotted with θ_s become tilted and almost horizontal above the level 600 hPa in Fig. 4 while it is above the level 300 hPa in Fig. 1 for θ'_w and in Fig. 3 for $\theta_{e/B73}$, or above 9000 m with $\theta_{e/MPZ}$ in MPZ. The isentropes computed with θ_s are therefore not compatible with the isolines of θ'_w or $\theta_{e/B73}$ and the more the relative humidity H_l is large in Fig. 2 the more the isentropes differ.

Similarly, the aim of the following sections is to show that varying values for r_v must have great impact on the definition and the plot of the isentropic surfaces considered in E86, E94 or MPZ. To do so, all the moist-air equivalent potential temperatures and the entropies given by Eqs. (1)-(13) are computed for a series of 15 points selected arbitrarily and plotted in Figs. 1-4. These 15 points describe a sort of Carnot cycle inspired by the one described in Emanuel (1986, 1991, 2004). The basic thermodynamic conditions (p , T , r_v , $q_l = q_i = 0$) of these points are listed in Table 1. The dry descent follows a path of almost constant relative humidity between 60 and 70 % (points 11 to 15), whereas the moist ascent follows a path of almost constant θ_s and

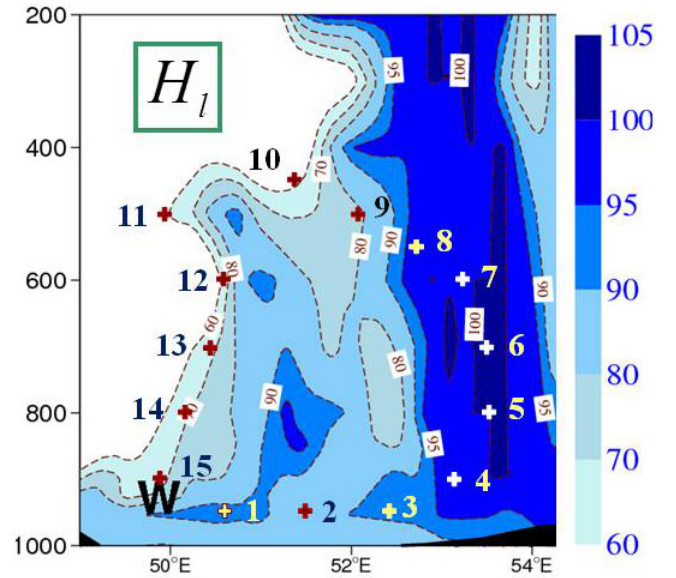


Figure 2: The same as in Fig. 1, but for the relative humidity H_l in %.

moist-air entropy (points 6 to 10).

The impact of condensed water and of non-equilibrium terms is expected to be smaller than impact due to changes in r_v . For the sake therefore of simplicity, the condensed water and the non-equilibrium effects are discarded (namely $T_l = T_i = T$ for the 15 points, with $H_l = H_i = 1$ and $q_l = q_i = 0$ in the just-saturated regions).

5 Impacts on potential temperatures

All moist-air potential temperatures given by Eqs. (1)-(7) are plotted in Fig. 5, with three of them listed in Table 1.

As can clearly be seen, $(\theta_s)_1$, $(\theta_s)_2$ and θ_s remain close to each other with an accuracy of ± 0.8 K for $(\theta_s)_1$, and with $(\theta_s)_2$ almost overlapping θ_s . This is proof that $(\theta_s)_1$ and $(\theta_s)_2$ are accurate increasing order approximations for θ_s .

The equivalent formulations $\theta_{e/MPZ}$, $\theta_{e/E94}$ and $\theta_{e/B73}$ exhibit large discrepancies, especially in the warm and moist ascent where differences of ± 2.5 K are observed between 950 and 700 hPa. Moreover, the dry descent for the saturated version $\theta_{es/E86}$ is 10 K warmer than that of other definitions of θ_e .

The differences between the five formulations are small at high levels: they are less than ± 3 K at 400 hPa, because $r_v = 2.84$ g kg $^{-1}$ is small. The impact is much larger at low level where $r_v > 15$ g kg $^{-1}$, with θ_s about 15 K colder than the ascent values of θ_e and θ_{es} at 950 hPa.

“Isentropic” surfaces or regions cannot therefore be the same if diagnosed through the use of values of either θ_s , θ_e or θ_{es} and the comparisons described in MPZ which are based on analyses of altitude- $\theta_{e/MPZ}$ diagrams (MPZ’s Figs. 4 and 6 to 9) might be invalid, since changes in the vertical may

Table 1: The pressure (in units of hPa), temperature (in units of K), water-vapor mixing ratios (in units of g/kg) and relative humidity (over liquid water, in units of %) for the 15 points depicted in Figs. 1-4. The potential temperature (in units of K) are the pseudo-adiabatic values (θ'_w), the third-law based values $\theta_{s/M11}$ computed by Eq. (5), the saturating equivalent values $\theta_{es/E86}$ computed by Eq. (2) and the equivalent values $\theta_{e/MPZ}$ computed by Eq. (4). The moist-air entropies (in units of $J K^{-1} kg^{-1}$) are: $s(\theta_{s/M11})$ computed by Eq. (8) with an offset of $-6850 J K^{-1} kg^{-1}$; $(s/q_d)(\theta_{es/E86})$ computed by Eq. (13) with an offset of $-5650 J K^{-1} kg^{-1}$; $(s/q_d)(\theta_{e/MPZ})$ computed by Eq. (11) with an offset of $+550 J K^{-1} kg^{-1}$.

N	p	T	r_v	H_l	θ'_w	$\theta_{s/M11}$	$\theta_{es/E86}$	$\theta_{e/MPZ}$	$s(\theta_{s/M11})$	$(s/q_d)(\theta_{es/E86})$	$(s/q_d)(\theta_{e/MPZ})$
1	950	295.10	16.25	91.9	296.32	329.17	345.36	339.33	112.4	222.0	783.3
2	950	296.56	16.24	84.1	296.71	330.80	351.29	340.93	117.4	239.2	788.3
3	950	296.12	17.45	92.6	297.41	332.48	349.34	343.21	122.5	233.6	796.8
4	900	294.07	17.11	97.5	297.85	334.72	348.84	345.21	129.2	232.1	802.7
5	800	290.16	15.41	99.9	298.28	338.48	350.30	347.98	140.4	236.3	809.5
6	700	285.08	12.64	100	298.01	340.29	350.15	348.24	145.8	235.9	807.3
7	600	278.05	8.94	98.2	296.95	339.74	347.39	345.57	144.2	228.0	795.3
8	550	273.57	6.90	95.9	296.16	338.71	345.23	343.30	141.1	221.7	786.4
9	500	270.03	4.87	80	295.58	339.52	346.65	342.81	143.5	225.8	782.9
10	450	265.38	2.84	60	294.85	339.69	346.88	341.65	144.0	226.5	777.5
11	500	268.89	3.35	60.1	293.90	335.01	343.87	337.33	130.1	217.7	765.0
12	600	277.15	5.95	70	294.39	332.87	345.19	336.90	123.7	221.6	766.1
13	700	282.52	7.40	70	293.45	327.41	342.33	332.41	107.0	213.2	753.5
14	800	286.59	8.49	70	292.18	321.66	338.42	327.40	89.2	201.7	738.6
15	900	292.28	10.90	70.1	292.85	321.50	342.54	328.73	88.8	213.8	744.8

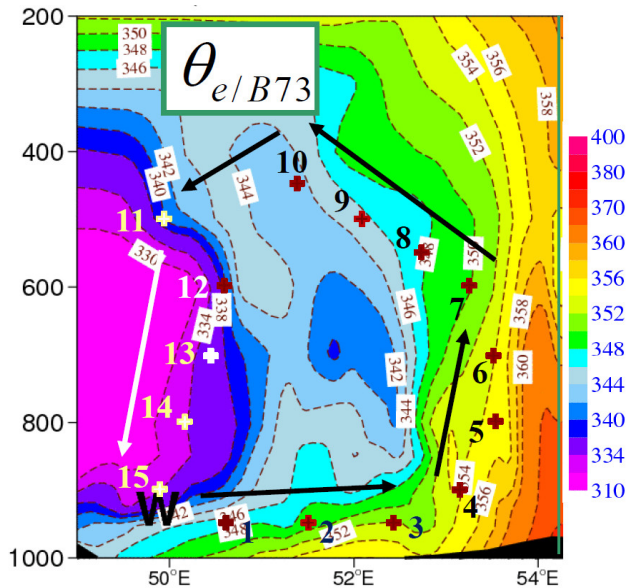


Figure 3: The same as in Fig. 1, but for the potential temperatures $\theta_{e/B73}$ in K computed by Eq. (3).

be of an opposite sign from the one for θ_s .

Indeed, the solid disks plotted in Fig. 5 and the corresponding values in Table 1 show that ascents between the levels 800 and 450 hPa correspond to a small increase in θ_s of +1.21 K while they correspond to a large decrease in $\theta_{e/MPZ}$ of -6.33 K. Such a relative difference of about 7.5 K is larger than the difference in equivalent potential temperatures of about 5 K between the properties of updrafts and

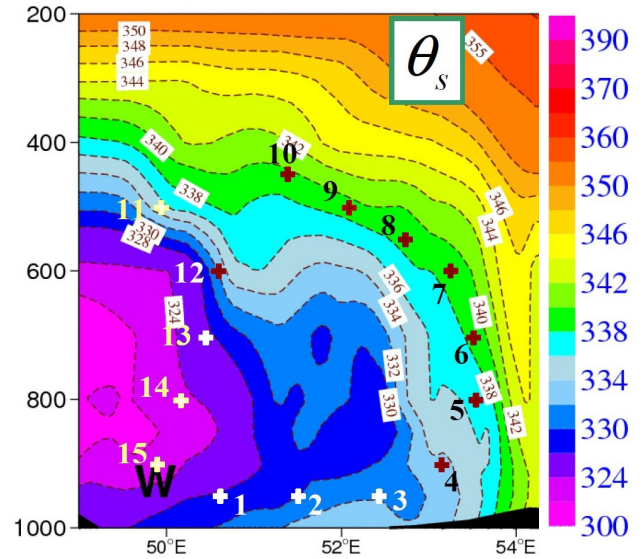


Figure 4: The same as in Fig. 1, but for the potential temperatures $\theta_{s/M11}$ in K computed by Eq. (5).

downdrafts described on page 1867 (right) in MPZ.

Another way in which to analyze the difference between θ_s and $\theta_{e/MPZ}$ or $\theta_{e/E94}$ is to consider the gap between descending and ascending values at 800 hPa: $\Delta\theta_s \approx 17$ K and $\Delta\theta_{e/MPZ} \approx \Delta\theta_{e/E94} \approx 21$ K. The difference is even larger for $\Delta\theta_{e/B73} \approx 24$ K. On the other hand, the difference is much smaller for $\Delta\theta_{es/E86} \approx 12$ K.

The important consequences of these findings is that changes in moist-air entropy represented by either θ_s or

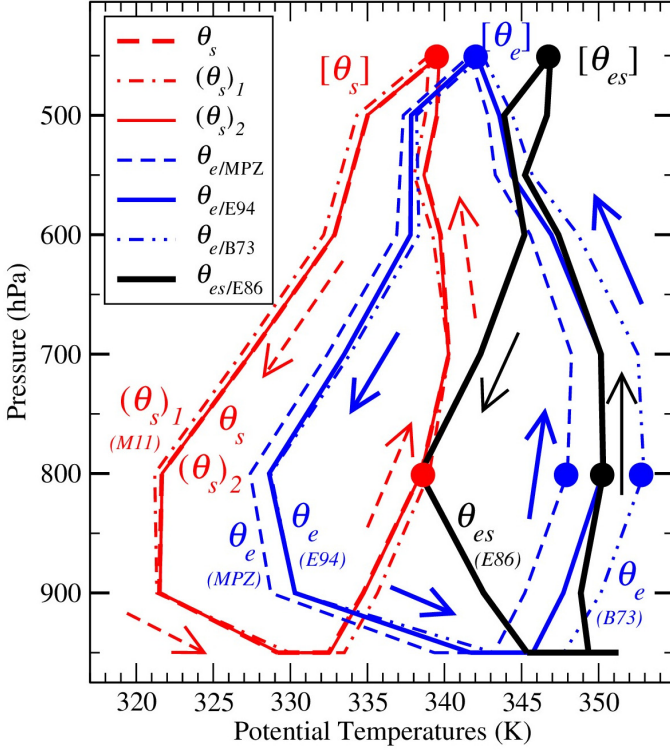


Figure 5: The seven potential temperatures given by Eqs. (1)-(7) (in K) are plotted against the pressure (in hPa) for the 15 points depicted in Figs. 1-4.

$\theta_{e/MPZ}$ cannot be simultaneously positive or negative, because otherwise it would be impossible to decide whether or not turbulence, convection or radiation processes would increase or decrease the moist-air entropy in the atmosphere. Moreover, since isentropic processes or changes in entropy must be observable facts, it is impossible to consider that all definitions given by Eqs. (1)-(7) are equivalent: at most only one of them can correspond to real atmospheric processes.

6 Impacts on moist-air entropies

The issue of computing the relevant moist-air entropy is even harder than choosing one of the equivalent potential temperatures studied in the previous section, namely either θ_s or one of the versions of θ_e or θ_{es} . Since the aim of MPZ and Emanuel (1986, 1991, 2004), Pauluis et al. (2010) or Pauluis (2011) is to analyze meteorological properties in moist-air isentropic coordinates, comparison of values of the moist-air entropy itself is needed. Let us therefore plot in the temperature-entropy diagram depicted in Fig. 6 the values of the six moist-air entropies considered in section 3.

The differences between the loops (Carnot cycles) are great. Some of the loops are very narrow, whereas others are wide with a flared shape (a large gap between ascending and descending regions). Some of the loops are almost vertical (with a small change of less than $\pm 20 \text{ J K}^{-1} \text{ kg}^{-1}$ in entropy between the surface and the upper air), whereas oth-

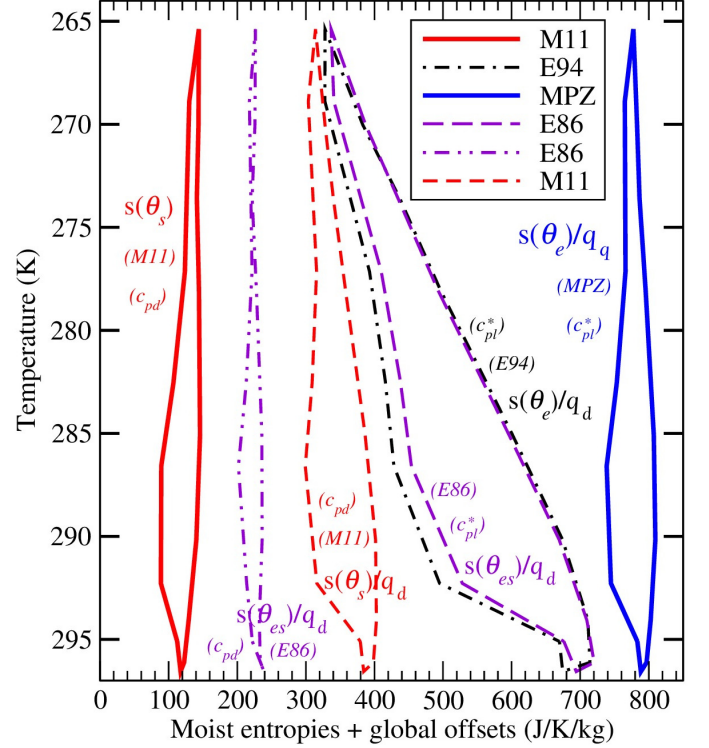


Figure 6: The 6 moist-air entropies (in units of $\text{J K}^{-1} \text{ kg}^{-1}$) defined by Eqs. (8)-(13) plotted in a same temperature-entropy diagram. Different global offsets are used for each entropy loop, in order to better separate and facilitate the comparison of the loops.

ers exhibit a pronounced tilted feature (with a large decrease of $400 \text{ J K}^{-1} \text{ kg}^{-1}$ between the warm and moist regions and the cold and dry ones).

Again, since isentropic processes or changes in entropy must be observable facts, it is impossible to consider that all definitions given by Eqs. (8) to (13) are equivalent: at most only one of them can correspond to real atmospheric processes.

Another way in which to analyze the difference between the various formulations for moist-air entropy is to compute the heat input W created by the closed loops in the temperature-entropy diagram, yielding

$$W = \oint T(s) ds. \quad (14)$$

Since W is measured by the area of the loops in Fig. 6, it is independent of the global offset chosen for each loop.

Values of W listed in Table 2 show that it is impossible to consider that one can choose one formulation or another. Since temperatures vary by about 30 K and for an accuracy of about $0.2 \text{ J K}^{-1} \text{ kg}^{-1}$ for entropies, errors in computations of W are about 6 J kg^{-1} . This means that the observed differences of the order of hundreds or thousands of J kg^{-1} are significant.

Table 2: The heat input W (in units of $J\ kg^{-1}$) given by Eq. (14) and computed for the six moist-air entropies considered in section 3. W represents the areas of the six loops depicted in Fig. 6. The wind scale $\sqrt{2W}$ is in units of $m\ s^{-1}$).

“ θ ”	$\theta_{es/E86}$	θ_s	θ_e/MPZ	θ_s	$\theta_{es/E86}$	$\theta_e/E94$
“ s ”	s/q_d	s	s/q_d	s/q_d	s/q_d	s/q_d
“ c_p ”	c_{pd}	c_{pd}	c_{pl}^*	c_{pd}	c_{pl}^*	c_{pl}^*
W	452	892	1213	1572	2871	3564
$\sqrt{2W}$	30.1	42.2	49.2	56.1	75.8	84.4

More precisely, large factors of 3 or 4 are observed between W computed with the third law value $s(\theta_s)$ and W computed with $s(\theta_{es/E86})/q_d$ or $s(\theta_e/E94)/q_d$. Furthermore, the impact of c_{pl}^* versus c_{pd} is very large, leading to a factor of more than 6 for the two heat inputs W computed with the same potential temperature $\theta_{es/E86}$ (452 versus 2871 $J\ kg^{-1}$).

The impact of the definitions “per unit of dry air” versus the specific ones (namely “per unit of moist air”) can be evaluated by comparing s and s/q_d for the same third law value $\theta_s/M11$. The impact $1572 - 892 = 680\ J\ kg^{-1}$ is great, leading to an increase of more than 75 % for the definition “per unit of dry air”.

The impact of the choice of the different formulations for the moist-air entropy can be evaluated differently, by computing the wind scale $W = V^2/2$, with V becoming a crude proxy for the surface wind that a perfect Carnot engine might produce. The last line in Table 2 shows that V would vary from about 30 to more than 80 $m\ s^{-1}$: this is unrealistic.

7 Conclusion

The isentropic analysis conducted in MPZ is likely a powerful tool for the investigation of moist-air energetics by the plotting of moist-air isentropes or by the computing of isentropic mass fluxes. The quality and the realism of such an analysis relies on a clear definition of the moist-air entropy however.

It is shown in this Comment that the way in which the potential temperatures θ_s , θ_e or θ_{es} are defined as “equivalents” of the moist-air entropy significantly impacts the computations and plots of isentropic surfaces, making the “isentropic” analyses similar to the one published in MPZ uncertain.

It is shown moreover that the heat input computed for loops in the Carnot cycle is largely modified not only by the choice of θ_s , θ_e or θ_{es} , but also by the way in which the entropy itself is defined: s or s/q_d ; modified reference values for entropies; c_{pd} or c_{pl}^* in factor of the logarithm; other missing terms; *etc*

As for the issue associated with the vision “per unit mass of dry air”, it can be understood as follows. If isentropic processes are defined as in E94 and MPZ with constant val-

ues of s/q_d , one should modify accordingly the definitions of the geopotential, the wind components or the kinetic energy by plotting for instance gz/q_d , u/q_d , v/q_d or $(u^2 + v^2)/(2q_d)$. These definitions are unusual. Moreover, if s/q_d could be defined within a global constant C , the specific value s would depend on $q_d C$, which varies with q_d and renders the integral $S = \iiint s\ \rho\ d\tau$ indeterminate, because it would depend on $\iiint q_d C\ \rho\ d\tau$ where C is an unknown term.

In conclusion, since moist-air isentropic surfaces are not subject to uncertainty in Nature, the third-law definitions θ_s and $s(\theta_s)$ given by Eqs. (5) and (8) are likely the more relevant, being as they are based on general thermodynamic principles and with specific values expressed per unit mass of moist air, as with all other variables in fluid dynamics.

References

- Betts, A. K., 1973: Non-precipitating cumulus convection and its parameterization. *Q. J. R. Meteorol. Soc.*, **99** (419), 178–196.
- Emanuel, K. A., 1986: An air-sea interaction theory for tropical cyclones. part i: Steady-state maintenance. *J. Atmos. Sci.*, **43** (6), 585–605, doi:10.1175/1520-0469(1986)043<0585:AASITF>2.0.CO;2.
- Emanuel, K. A., 1991: The theory of hurricanes. *Annu. Rev. Fluid Mech.*, **23** (1), 179–196, doi:10.1146/annurev.fl.23.010191.001143.
- Emanuel, K. A., 1994: *Atmospheric convection*, 580 pp. Oxford University Press, Incorporated.
- Emanuel, K. A., 2004: Dissipative heating and hurricane intensity. *Atmospheric Turbulence and Mesoscale Meteorology*, E. Fedorovich, R. Rotunno, and B. Stevens, Eds., Cambridge University Press, 280 pp.
- Hawkins, H. F., and S. M. Imbembo, 1976: The structure of a small, intense hurricane—Inez 1966. *Mon. Wea. Rev.*, **104** (4), 418–442, doi:10.1175/1520-0493(1976)104<0418:TSOASI>2.0.CO;2.
- Marquet, P., 2011: Definition of a moist entropy potential temperature: application to FIRE-I data flights. *Quart. J. Roy. Meteorol. Soc.*, **137** (9), 768–791, doi:10.1002/qj.787.
- Marquet, P., 2015: An improved approximation for the moist-air entropy potential temperature θ_s . *Research Activities in Atmospheric and Oceanic Modelling. WRCP-WGNE Blue-Book*, **4**, 14–15, URL <http://arxiv.org/abs/1503.02287>, http://www.wcrp-climate.org/WGNE/BlueBook/2015/chapters/BB_15_S4.pdf.
- Marquet, P., 2016: The mixed-phase version of moist-entropy. *Research Activities in Atmospheric*

and *Oceanic Modelling. WRCP-WGNE Blue-Book*, **4**, 7–8, URL <http://arxiv.org/abs/1605.04382>, http://www.wcrp-climate.org/WGNE/BlueBook/2016/documents/Sections/BB_16_S4.pdf.

Marquet, P., and J.-F. Geleyn, 2015: Formulations of moist thermodynamics for atmospheric modelling. *Parameterization of Atmospheric Convection. Vol II: Current Issues and New Theories*, R. S. Plant, and J.-I. Yano, Eds., *World Scientific*, Imperial College Press, 221–274, doi:10.1142/9781783266913_0026, URL <http://arxiv.org/abs/1510.03239>.

Mrowiec, A. A., O. M. Pauluis, and F. Zhang, 2016: Isentropic analysis of a simulated hurricane. *J. Atmos. Sci.*, **73** (5), 1857–1870, doi:10.1175/JAS-D-15-0063.1.

Pauluis, O., 2011: Water vapor and mechanical work: A comparison of carnot and steam cycles. *J. Atmos. Sci.*, **68** (1), 91–102, doi:10.1175/2010JAS3530.1.

Pauluis, O., A. Czaja, and R. Korty, 2010: The global atmospheric circulation in moist isentropic coordinates. *J. Climate*, **23** (11), 3077–3093, doi:10.1175/2009JCLI2789.1.